

## Testing and modelling of hardwood joints using beech and azobé

Sandhaas, Carmen; Khaloian Sarnaghi, A.; van de Kuilen, J.W.G.

**Publication date**

2019

**Document Version**

Final published version

**Published in**

ISCHP 2019 - 7th International Scientific Conference on Hardwood Processing

**Citation (APA)**

Sandhaas, C., Khaloian Sarnaghi, A., & van de Kuilen, J. W. G. (2019). Testing and modelling of hardwood joints using beech and azobé. In J.-W. van de Kuilen, & W. Gard (Eds.), *ISCHP 2019 - 7th International Scientific Conference on Hardwood Processing* (pp. 85-92). Delft University of Technology.

**Important note**

To cite this publication, please use the final published version (if applicable).  
Please check the document version above.

**Copyright**

Other than for strictly personal use, it is not permitted to download, forward or distribute the text or part of it, without the consent of the author(s) and/or copyright holder(s), unless the work is under an open content license such as Creative Commons.

**Takedown policy**

Please contact us and provide details if you believe this document breaches copyrights.  
We will remove access to the work immediately and investigate your claim.

## Testing and modelling of hardwood joints using beech and azobé

C. Sandhaas<sup>1\*</sup>, A. Khaloian Sarnaghi<sup>2</sup>, and J.W.G. van de Kuilen<sup>2,3</sup>

<sup>1</sup>Timber Structures  
Karlsruhe Institute of Technology  
76131 Karlsruhe, Germany

<sup>2</sup>Wood Technology  
Technical University of Munich  
80797 Munich, Germany

<sup>3</sup>Biobased Structures and Materials  
Delft University of Technology  
2628 CN Delft, the Netherlands

### ABSTRACT

*Tests on double-shear steel-to-timber joints loaded parallel-to-grain were undertaken, using beech and azobé with one, three and five dowels in a row. The dowels were made of high strength steel (hss) and very high strength steel (vhss). The experiments have shown a significant difference in load-carrying capacity of joints with vhss and hss dowels. Joints with one dowel provided enough plastic deformation capacity to allow for ductile failure modes whilst this does not hold for joints with three or five dowels in a row. No correlation between load-carrying capacity and density within one wood species could be observed. Novel failure modes including steel failure of the dowels were observed. The observed effective number of fasteners was lower for the joints with vhss dowels. Also for the stiffness  $K_{ser}$ , an effective number of fasteners could be observed. The tested timber joints with their simultaneous ductile and brittle failure modes still present a major challenge for modelling. Wood is heterogeneous, highly anisotropic and shows ductile behaviour in compression and brittle behaviour in tension and shear. A bespoke 3D constitutive model for wood based on continuum damage mechanics was used to capture these effects. Eight stress-based failure criteria were defined in order to formulate piecewise defined failure surfaces. The damage development was controlled by nine damage variables that were inserted in the damage operator. The joint test results were compared to modelling outcomes. The failure modes could be identified and the general shape of the load-displacement curves agreed with the experimental outcomes.*

### 1. INTRODUCTION

In timber joints with dowel-type fasteners, the preferred failure mode is combined failure of yielding of the fastener and embedment of the timber. Apart from the geometry, the load-carrying capacity is therefore defined by the embedment strength of the timber and the yield moment of the dowel-type fastener. The utilisation of very high strength steels (vhss) with subsequent higher yield moments is promising in order to optimise joints and get high performance connections. Thinner dowels and thinner member sections should lead to the same load-carrying capacity as have thicker mild steel dowels with bigger member cross sections – as long as failure modes with one or two plastic hinges per shear plane is reached. Another option is that with the same dimensions, fewer dowels could be used to obtain the same performance. This is especially valid and even more advantageous for high-density timber. The embedment strength of species with high densities is higher. Therefore, less member thickness would be needed when using vhss dowels in high-density timber in comparison to softwood. In the Netherlands, tropical hardwood with high densities is used for bridges and waterworks such as lock gates or mooring posts. The practical applicability is hence guaranteed

Tests have been carried out on double-shear steel-to-timber connections with vhss dowels using beech (*Fagus sylvatica*) and azobé (*Lophira alata*) (Sandhaas and van de Kuilen 2016). Comparative tests were done on the same connections, but with lower steel grade dowels. The dowel diameters were 12 and 24 mm. The number of dowels in a row was one, three and five. No other parameters such as further species, other dowel diameters or joint layout were experimentally evaluated. For this, in general, parametric studies applying finite element methods are used. However, timber joints are difficult to model. Apart from heterogeneity, two other main material-specific issues lead to numerical problems: anisotropy with different strength in tension and compression and ductile and brittle failure modes occurring simultaneously. Within the framework of continuum damage mechanics (CDM), a general approach combining the above-mentioned issues in one single 3D material model (Sandhaas 2012) was applied to predict the joint behaviour. Particularly, the capability of the models to capture failure modes was assessed.

\* Corresponding author; E-mail: sandhaas@kit.edu

## 2. EXPERIMENTAL PROGRAMME

### 2.1. TEST SETUP

A total of 120 tests on steel-to-timber joints loaded parallel-to-grain were carried out varying the parameters wood species, dowel diameter, steel grade and number of dowels in a row. Figure 1 gives an overview of the test series. The end and edge distances and the spacing of the dowels are given in Figure 2. They comply with the minimum requirements of Eurocode 5 (2010). The member thickness  $t$  given in Table 1 was designed such that the failure modes of the joints with vhss dowels were expected to lie between one and two plastic hinges per shear plane (see Figure 6). Subsequently, the joints with hss dowels should clearly fail with two plastic hinges per shear plane. The test setup is shown in Figure 2 where only the lower joint is relevant, the upper joint served to fasten the specimen in the test rig. Tensile tests on the used steel dowels were carried out. The hss dowels had a mean tensile strength of 640 MPa (12 mm dowels) and 540 MPa (24 mm dowels), which is considerably higher than the characteristic strength of 360 MPa for the ordered steel grade S235. The vhss dowels had a tensile strength of 1400 MPa (12 mm dowels) and 1380 MPa (24 mm dowels).

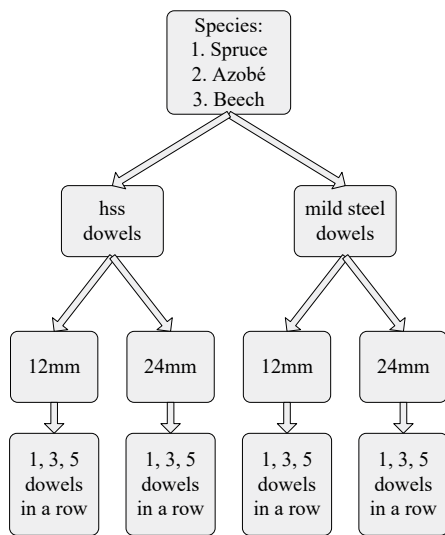


Figure 1: Flowchart of tests, 5 tests per series



Figure 2: Typical test specimen, here with three dowels

The used wood species were the European species beech (*Fagus sylvatica*) and azobé (*Lophira alata*) as a high-density tropical hardwood species. The beech members were made of glulam due to the necessary large cross sections and they were stored at a normal climate (20°C and 65% relative humidity). The azobé members were stored at a climate with 20°C and 85% relative humidity. The resulting moisture contents  $u$  (determined after the tests with the oven-dry method) can be taken from Table 1, where also the values for the densities  $\rho_d$  are given. Reported densities are calculated as the mean value of the individual members of a joint. All tests were carried out following the protocol from EN 26891 (1991) with an initial unloading loop after reaching 40% of the estimated maximum load  $F_{max}$ . The tests were continued up to final failure. All specimens were loaded in tension as shown in Figure 2. The relative slip between outer timber members and the central steel plate was measured with four LVDTs, one on front and rear of each outer timber member, see also Figure 2.

### 2.2. TEST RESULTS

The test results in terms of mean values are given in Table 1. Figures 3 and 4 show the load-slip curves for the tests on joints with beech members and 24 mm dowels and with azobé members and 12 mm dowels. All test specimens failed with one plastic hinge per shear plane (vhss dowels) or with two plastic hinges per shear plane (hss dowels) except for three specimens with five 24 mm vhss dowels in a row that failed without plastic hinges in the dowels. The deformation angles of the dowels were measured. Analogously to Jorissen (1998), bending angles of 45° were never reached. The measured mean bending angle of the joints with one dowel was 10°, which decreased significantly for the joints with three and five dowels in a row where bending angles between 1° and 5° could be observed. For these multiple dowelled joints, the bending angles of the hss dowels were consistently bigger than the angles for vhss dowels.

## Testing and modelling of hardwood joints using beech and azobé

 Table 1: Test series (5 tests per series) and results in terms of mean values (coefficients of variation are given in parentheses).  
 $t$  = thickness of timber members,  $u$  = moisture content,  $\rho_u$  = density at  $u$ ,  $F_{max}$  = maximum load per joint (i.e. per two shear planes),  
 $v$  = displacement at  $F_{max}$ ,  $k_s$  = initial stiffness acc. to EN 26891 (1991)

| Diameter [mm] | Species | $t$ [mm] | No. of dowels | Steel grade | $\rho_u$ [kg/m <sup>3</sup> ] | $u$ [%]     | $F_{max}$ [kN] | $F(vhss)/F(hss)$ | $v$ at $F_{max}$ [mm] | $k_s$ [kN/mm] |
|---------------|---------|----------|---------------|-------------|-------------------------------|-------------|----------------|------------------|-----------------------|---------------|
| 12            | Beech   | 72       | 1             | vhss        | 722 (2.5)                     | 8.7 (3.1)   | 70 (6.0)       | 1.18             | 15.9 (14.6)           | 49 (44.2)     |
|               |         |          |               | hss         | 720 (1.6)                     | 8.6 (3.4)   | 59 (3.6)       |                  | 15.5 (7.2)            | 36 (40.6)     |
|               |         |          | 3             | vhss        | 732 (4.8)                     | 8.7 (1.4)   | 173 (4.9)      | 1.10             | 6.5 (34.9)            | 67 (8.4)      |
|               |         |          |               | hss         | 730 (2.2)                     | 8.5 (0.7)   | 157 (4.6)      |                  | 5.9 (23.2)            | 61 (28.8)     |
|               |         |          | 5             | vhss        | 703 (2.3)                     | 8.5 (1.0)   | 294 (2.5)      | 1.22             | 5.3 (17.4)            | 129 (13.3)    |
|               |         |          |               | hss         | 718 (3.1)                     | 8.8 (12.6)  | 240 (2.5)      |                  | 4.5 (8.8)             | 110 (4.2)     |
|               | Azobé   | 65       | 1             | vhss        | 1115 (2.3)                    | 22.0 (1.4)  | 72 (2.7)       | 1.26             | 7.9 (17.1)            | 53 (12.4)     |
|               |         |          |               | hss         | 1115 (2.3)                    | 21.4 (1.4)  | 57 (6.5)       |                  | 11.1 (41.1)           | 45 (29.5)     |
|               |         |          | 3             | vhss        | 1131 (4.0)                    | 22.9 (3.1)  | 183 (7.9)      | 1.43             | 4.8 (23.4)            | 64 (11.2)     |
|               |         |          |               | hss         | 1117 (1.4)                    | 21.8 (0.9)  | 128 (7.6)      |                  | 3.7 (35.7)            | 39 (6.7)      |
|               |         |          | 5             | vhss        | 1130 (3.9)                    | 17.2 (2.4)  | 281 (13.2)     | 1.21             | 2.9 (15.3)            | 158 (22.1)    |
|               |         |          |               | hss         | 1115 (1.6)                    | 21.7 (0.8)  | 233 (14.1)     |                  | 4.0 (56.1)            | 132 (6.0)     |
| 24            | Beech   | 144      | 1             | vhss        | 710 (1.0)                     | 8.5 (2.0)   | 300 (2.4)      | 1.44             | 20.0 (21.8)           | 157 (7.7)     |
|               |         |          |               | hss         | 719 (2.2)                     | 8.7 (8.0)   | 208 (3.6)      |                  | 23.8 (16.2)           | 114 (20.4)    |
|               |         |          | 3             | vhss        | 724 (0.9)                     | 8.3 (1.3)   | 659 (5.1)      | 1.29             | 4.2 (12.4)            | 205 (2.9)     |
|               |         |          |               | hss         | 711 (1.7)                     | 8.4 (0.8)   | 510 (5.0)      |                  | 6.0 (29.4)            | 202 (17.2)    |
|               |         |          | 5             | vhss        | 695 (2.3)                     | 9.4 (4.5)   | 927 (3.5)      | 1.13             | 4.1 (13.5)            | 192 (6.3)     |
|               |         |          |               | hss         | 701 (1.0)                     | 9.8 (2.9)   | 823 (5.3)      |                  | 6.5 (24.0)            | 171 (7.2)     |
|               | Azobé   | 120      | 1             | vhss        | 1154 (1.9)                    | 21.5 (3.1)  | 306 (6.4)      | 1.69             | 5.3 (28.2)            | 201 (17.5)    |
|               |         |          |               | hss         | 1123 (3.1)                    | 21.5 (5.9)  | 181 (10.6)     |                  | 15.3 (36.8)           | 103 (15.1)    |
|               |         |          | 3             | vhss        | 1116 (1.9)                    | 21.3 (6.6)  | 706 (5.5)      | 1.31             | 4.2 (14.7)            | 246 (13.8)    |
|               |         |          |               | hss         | 1104 (2.3)                    | 22.6 (10.7) | 539 (7.2)      |                  | 5.0 (24.7)            | 186 (33.3)    |
|               |         |          | 5             | vhss        | 1111 (1.3)                    | 15.9 (15.7) | 1128 (16.0)    | 1.30             | 3.5 (36.9)            | 374 (40.9)    |
|               |         |          |               | hss         | 1118 (2.4)                    | 22.5 (6.9)  | 868 (11.0)     |                  | 4.9 (26.3)            | 321 (16.8)    |

Generally, dowels in joints with five dowels in a row were partly able to deform plastically before failure, especially when higher-density wood species were used. The displacement at the maximum load is however small. The joints with vhss dowels reached higher load-carrying capacities than the joints with hss dowels, see Table 1. The proportional limit of the joints with hss dowels is reached at lower loads than the one of the joints with vhss dowels. The ratios for the beech specimens with 12 mm dowels were however lower than expected. In order to consider all possible issues including the dowels, additional tension tests on 12 mm hss dowels were carried out. They showed that the hss dowels used for the beech specimens had 43% higher mechanical properties than the dowels for the azobé specimens, which explains why the trend of about 30% higher load-carrying capacity with vhss dowels was not found for this subseries. Finally, if the ordered mild steel grade dowels would have had a characteristic tensile strength of 360 MPa, the results given in Table 1 would have been more advantageous for the joints with vhss dowels. Then, an additional increase of the ratio of the load carrying capacities of about 40% would have been possible.

The joints with both species reach similar load-carrying capacities although the respective densities differ significantly. The moisture content of azobé was considerably higher than that of beech, which explains, at least partly, the similar values. Figures 3 and 4 show that the beech joints generally reach higher ultimate displacements compared to azobé, even though the differences disappear for three and five dowels in a row. For single dowel joints of beech, a large deformation capacity was observed with a consistent slight hardening. This also explains the relatively high load-carrying capacities of the beech joints. If for instance the load-carrying capacities of azobé and beech joints with one 12 mm vhss dowel are compared at the same displacement of 5 mm, i.e. 70 kN for beech joints and 72 kN for azobé joints, the ratio of the load-carrying capacities changes to 1.16 instead of  $72/70 = 1.03$ . Generally, beech is a ductile wood species that is able to support higher deformations before splitting than other species. This confirms earlier

research on the embedment strength of beech where high ductility, depending on the annual ring layout (reinforcement through rays), was observed (Sandhaas et al. 2013).

Figure 5 shows the dependency of the load-carrying capacity on the density of the timber members. A uniform load and stiffness distribution between the single dowels has been assumed. Generally, within species, density variations are such that hardly any correlation is found between the density of timber members and the load-carrying capacity of timber joints produced from them. Apparently, the scatter in load-carrying capacities is caused not only by density, but, probably more important, variations in shear and splitting strength around the fasteners which have higher coefficients of variation than density.

Figure 6 finally shows typical failure modes of joints where the shown plastic deformation of the dowel was much less for joints with three or five dowels in a row. As can be also seen in the load-displacement curves given in Figures 3 and 4, those multiple dowelled joints failed at small displacements through splitting of the timber members. Furthermore, novel failure modes were observed that do not occur when using softwoods (Blass et al. 2017).

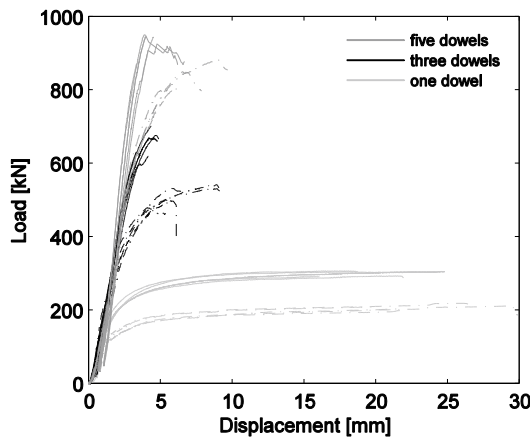


Figure 3: Mean load-displacement curves for beech joints with 24 mm dowels, solid line: vhss dowels, dashed line: hss dowels

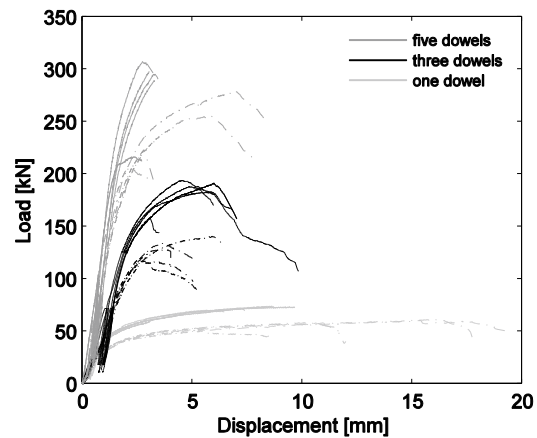


Figure 4: Mean load-displacement curves for azobé joints with 12 mm dowels, solid line: vhss dowels, dashed line: hss dowels

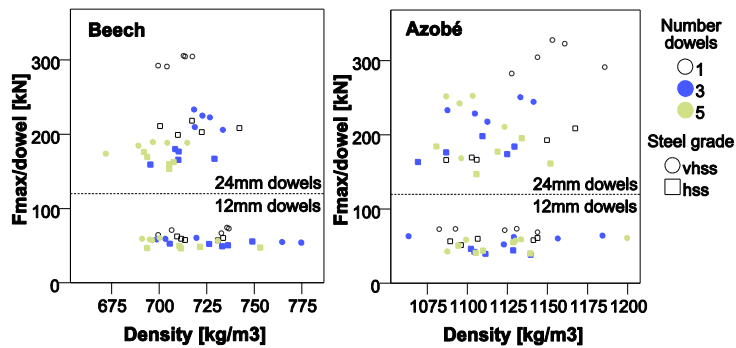


Figure 5: Density versus maximum load per dowel.

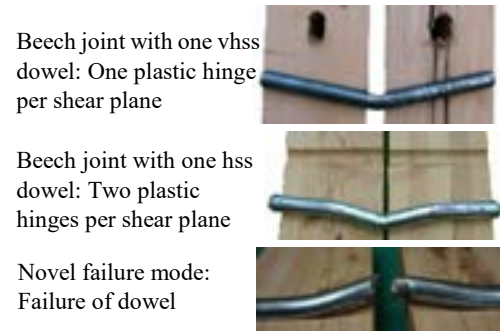


Figure 6: Failure modes of dowels.

### 3. MODELLING

#### 3.1 CONSTITUTIVE MODEL

As stated in the introduction, timber joints are difficult to model due to material anisotropy, simultaneous ductile and brittle failure modes and complex stress states around fasteners. In order to investigate the potential of a constitutive model for wood based on continuum damage mechanics (Sandhaas 2012) to represent stress states and failure modes, the tests presented in section 2 were modelled using this constitutive model.

Continuum damage mechanics (CDM) is a nonlinear elastic approach where the nonlinear behaviour is obtained by modifying the stiffness matrix  $\mathbf{D}$  or its inverse, the compliance matrix  $\mathbf{C}$ . CDM can be implemented in an incremental-iterative FE framework. The stress increments are calculated from strain increments via a variable stiffness matrix. Therefore and as opposed to classical plasticity, the unloading in damage mechanics is following the secant stiffness and not following the elastic stiffness. In CDM, a damage variable  $d$ ,  $0 \leq d \leq 1$ , is determined and inserted into the fundamental Hooke equation as follows:

$$\sigma_{ij} = (1-d) \cdot D_{ijkl} \cdot \varepsilon_{ij} \quad (1)$$

where  $\sigma_{ij}$  = stress matrix,  $d$  = damage variable,  $D_{ijkl}$  = stiffness matrix,  $\varepsilon_{ij}$  = strain matrix

If  $d = 0$ , no damage is present; if  $d = 1$ , the material has failed, where  $d$  is a scalar. However, anisotropic damage is observed for wood, which means that several damage variables  $d_{ij}$  must be defined to represent the 3D behaviour of wood. Therefore, three major mathematical definitions need to be established:

- Failure criteria to identify damage initiation;
- The post-elastic behaviour when  $0 \leq d \leq 1$ ;
- A constitutive model linking the stresses to the strains.

Damage initiation of timber depends on the material directions. For instance, damage due to exceedance of tensile strength perpendicular to the grain starts at a much lower level than damage due to exceedance of tensile strength parallel to the grain. Therefore, **piecewise defined failure criteria** were used to identify damage initiation where maximum stress criteria were used in the directions parallel to the grain and quadratic criteria in the direction perpendicular to the grain. Apart from the anisotropy of timber, also failure modes differ. For instance, damage due to exceedance of tensile strength perpendicular to the grain is brittle whereas the exceedance of compressive strength perpendicular to the grain leads to ductile behaviour. Therefore, **two simplified damage laws** were defined as shown in Figure 7 and 8 where the elastic-perfectly plastic law was applied for behaviour in compression and the brittle law for behaviour in tension and shear. The final **constitutive model** is given in Eq. (2) where the damaged compliance matrix  $\mathbf{C}^{dam}$  is shown.

$$\mathbf{C}^{dam} = \begin{bmatrix} \frac{1}{(1-d_0)E_L} & -\frac{\nu_{RL}}{E_R} & -\frac{\nu_{TL}}{E_T} & 0 & 0 & 0 \\ -\frac{\nu_{LR}}{E_L} & \frac{1}{(1-d_{90})E_R} & -\frac{\nu_{TR}}{E_T} & 0 & 0 & 0 \\ -\frac{\nu_{LT}}{E_L} & -\frac{\nu_{RT}}{E_R} & \frac{1}{(1-d_{90})E_T} & 0 & 0 & 0 \\ 0 & 0 & 0 & \frac{1}{(1-d_\nu)G_{LR}} & 0 & 0 \\ 0 & 0 & 0 & 0 & \frac{1}{(1-d_\nu)G_{LT}} & 0 \\ 0 & 0 & 0 & 0 & 0 & \frac{1}{(1-d_r)G_{RT}} \end{bmatrix} \quad (2)$$

where:

Indices  $L$ ,  $R$  and  $T$  refer to the longitudinal ( $L$ ), radial ( $R$ ) and tangential ( $T$ ) material directions;

Indices 0, 90,  $\nu$  and  $r$  identify damage parallel (0) and perpendicular (90) to the grain, in longitudinal ( $\nu$ ) and rolling shear ( $r$ ),

$E$  = moduli of elasticity

$G$  = shear moduli

$d$  = damage variables

$\nu$  = Poisson coefficients; were set to zero to avoid Poisson effects

For a through explanation of the constitutive model, please refer to Sandhaas (2012).



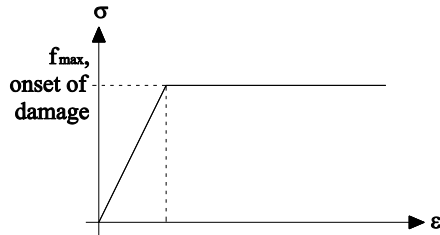


Figure 7: Elastic-perfectly plastic behaviour

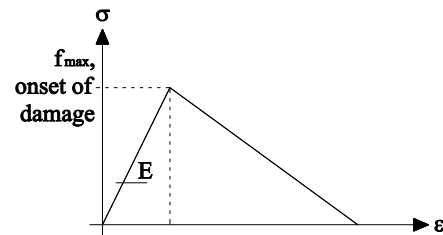


Figure 8: Brittle behaviour

### 3.2 MATERIAL PROPERTIES

A major issue of all material models is the need of mechanical input parameters such as stiffness and strength values that are usually based on test results. The developed model needs the mechanical input properties given in Table 2 per species. Generally, stiffness values are rather easily assembled with a satisfying reliability whereas already seemingly easy parameters as uniaxial strength values can be procured only with difficulty. This is due to two main issues. Firstly, the inherent large scatter of mechanical properties for timber and secondly, difficulties connected with testing and measuring. For instance, the uniaxial shear strength can hardly be assessed without triggering stress peaks or secondary stresses (Moses and Prion 2004). Furthermore, not always all parameters are measured, e.g. due to Poisson effect, or the positioning of the measuring instruments is not clear. In addition, the fracture energies suffer from a large scatter and they are usually derived from tests using small clear wood specimens which means that the heterogeneous nature of timber is not taken into account. Moreover, the needed material values are rather easily procurable for softwoods, but not for hardwoods.

Table 2: Material properties used in FE analysis

| Parameters                                      | Beech | Azobé | Parameters             | Beech | Azobé |
|---|-------|-------|------------------------|-------|-------|
| <b>Stiffness in MPa</b>                         |       |       | <b>Strength in MPa</b> |       |       |
| $E_L$   | 13000 | 20000 | $f_{i,0}$              | 86    | 72    |
| $E_R = E_T$                                     | 860   | 1330  | $f_{c,0}$              | 50    | 69    |
| $G_{LR} = G_{LT}$                               | 810   | 1250  | $f_{i,90}$             | 1.0   | 1.0   |
| $G_{RT}$  | 59    | 91    | $f_{c,90}$             | 14.2  | 23.2  |
| <b>Fracture energy <math>G_f</math> in N/mm</b> |       |       | $f_v$                  | 13    | 16    |
| $G_{f,parallel}$                                | 100   | 180   | $f_r$                  | 1.0   | 1.6   |
| $G_{f,perpendicular}$                           | 0.71  | 0.71  |                        |       |       |
| $G_{f,shear}$                                   | 1.2   | 1.5   |                        |       |       |
| $G_{f,rolling\ shear}$                          | 0.6   | 0.7   |                        |       |       |

### 3.3 JOINT MODELS

Double-shear steel-to-timber joint models with hss or vhss dowels have been created. Here, only models with one 12 mm dowel are presented. Von Mises plasticity with isotropic hardening has been used for all steel parts. Steel properties were a Poisson coefficient of 0.3, a modulus of elasticity of 21000 GPa, a yield strength of 570 MPa and a tensile strength of 600 for hss dowels and a yield strength of 1310 MPa and a tensile strength of 1350 MPa for vhss dowels. An exemplary joint model with one dowel is shown in Figure 9. The previously introduced constitutive model has been used only for the timber area surrounding the dowel (“UMAT” in Figure 9); in all other timber parts of the joint linear-elastic, orthotropic properties were used, applying the stiffness values given in Table 2. In the model, symmetry was used and only a quarter of the joint was modelled.

Joint models are complex models as they feature different contact regions; i.e. steel dowel/timber, steel plate timber and steel dowel/steel plate. Due to the significantly different moduli of elasticity of steel and timber, contact between these two materials is difficult to model. Deletion of the finite elements, after they have lost their stiffness, is making the damage propagation possible. However, as failure of the material generally occurs in the contact region between timber

and steel dowel, element deletion may lead to the deletion of the contact surface between steel and timber, which causes convergence problems. Therefore, element deletion in these models cannot be completed, and a tolerance needs to be defined, which reduces the stiffness of the elements without setting it to zero. Moreover, by restarting the mesh in every step, the failed elements in the contact region are removed and the contact surface is reactivated. Thus, the stiffness of the damaged elements is reduced, which deactivates the failed elements from taking the load and correspondingly prevents any stress transfer between these elements. Additionally, due to the contact problems in contact regions, the elements may get too rigid to deform flexibly to be able to reach a higher global displacement level. Therefore, the focus of this study is to overcome the problem of getting higher stiffness in the model and to come to a solution, which is able to predict the load-carrying capacity and the plastic behaviour of the material. General static solver and 3D linear hexahedral finite elements with reduced integration are used.

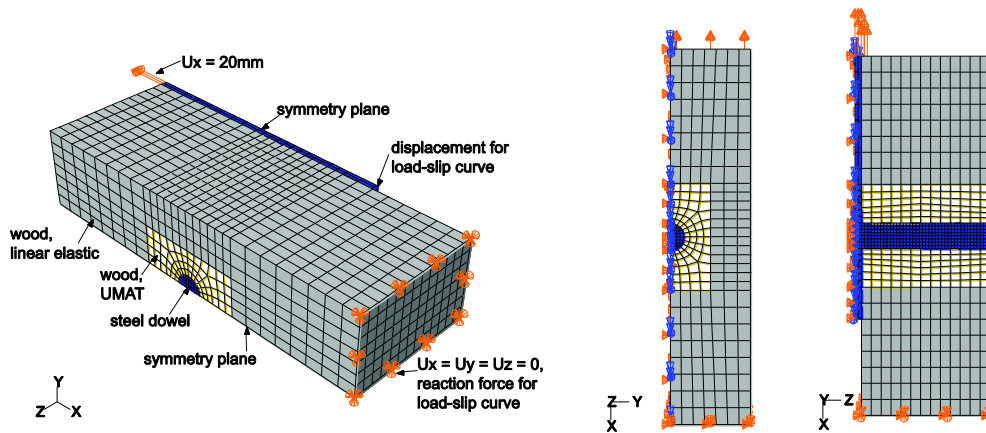


Figure 9: Typical model with one dowel, default mesh and boundary conditions.

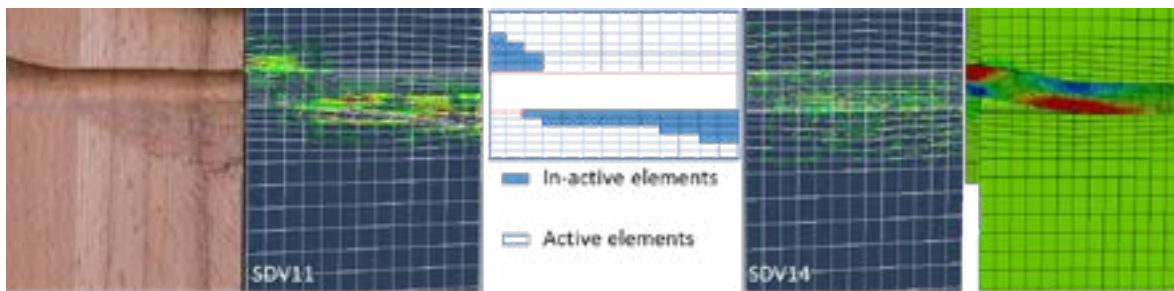


Figure 10: Typical modelling results for a joint with one hss dowel. From left to right: Photo after test, damage variable  $d_{c,0}$  = compression parallel to the grain (SDV11), identification of active and deleted elements,  $d_{t,90}$  = tension perpendicular to the grain (SDV14), stress in dowel axis direction

Figure 9 shows the sketch of the joint model with applied boundary conditions. Figure 10 shows results that help to judge the quality of the simulation. The results given in terms of damage variable  $d_{c,0}$  (damage due to compression parallel to the grain) show the fibre crushing underneath the dowel. The test result in this figure illustrates the good phenomenological agreement between model and test. The deleted elements are also identified, and they fit well to the test result. Lastly, the normal stresses in dowel axis direction are shown to visualise dowel bending.

Figures 11 and 12 give some modelling results superposed with experimental results. The simulations were carried out for three grades of steel dowels; adding mild steel dowels with a tensile strength of 350 MPa to the analyses. The numerical results for both beech and azobé are in good agreement with the experimental results regarding the stiffness. Regarding the load-carrying capacity, the experimental results for azobé are in the same range as the numerical results if the used steel strength in the models is one grade lower than the one used in the tests. This means that the numerical results of timber joints with dowels of 600 MPa strength correspond well with the experimental results with dowels of 1350 MPa strength, and 350 MPa strength of steel dowels in numerical results correspond well with 600 MPa steel dowels in experiments. This is notable as not always tensile tests on fasteners are carried out and hence, numerical results using nominal values are compared to experimental results, which, in this case would lead to good overlap as mild steel dowels of grade S235 have been ordered.



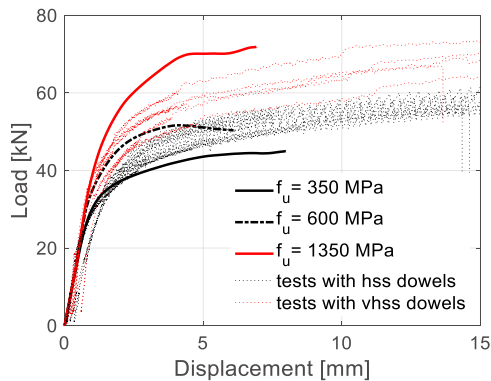


Figure 11: Overlap of numerical and experimental results for beech joints

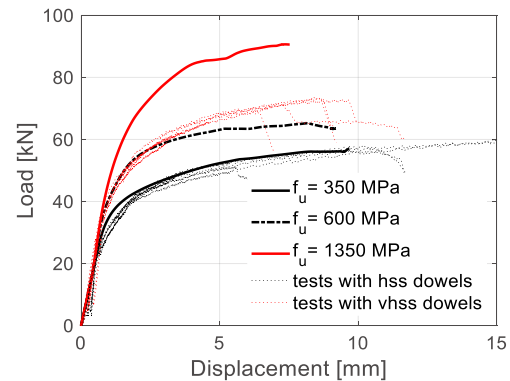


Figure 12: Overlap of numerical and experimental results for azobé joints

## 6. SUMMARY

The test results confirmed the feasibility of using very high strength dowels in timber joints. The load-carrying capacity of the joints with vhss dowels were increased by 10% to 69% in comparison to the same joints with hss steel dowels. Ductile failure modes with one or two plastic hinges per shear plane were possible. The tested joints were modelled using a bespoke constitutive model for the material timber that can identify failure modes and combine simultaneous ductile and brittle failures within one model. The mechanical material parameters needed for the constitutive relationship are clearly defined. The material model runs in a complex FE environment in combination with other material models and contact formulations. Modelling results were satisfying in terms of stiffness and load-carrying capacity. As for any other modelling approach, a major issue lies in the determination of the necessary mechanical properties. As the model performance and prediction capacity is highly dependent on these properties, methods to derive reliable values must be developed.

## ACKNOWLEDGEMENTS

We thank the companies *Pollmeier Massivholz GmbH & Co KG* for donating the beech wood and *Groot Lemmer* for sponsoring and manufacturing the azobé specimens.

## REFERENCES

- Blass, H.J., C. Sandhaas and N. Meyer. 2017. *Steel-to-timber connections: Failure of laterally loaded dowel-type fasteners. Proceedings INTER Meeting 49, Paper 50-7-1, Kyoto, Japan. Pages 67-79.*
- EN 1995 1-1:2010. *Eurocode 5. Design of timber structures - Part 1-1: General - Common rules and rules for buildings. Comité Européen de Normalisation (CEN), Brussels, Belgium.*
- EN 26891:1991. *Timber structures - Joints made with mechanical fasteners - General principles for the determination of strength and deformation characteristics (ISO 6891). Comité Européen de Normalisation (CEN), Brussels, Belgium.*
- Jorissen, A. 1998. *Double-shear timber connections with dowel-type fasteners. PhD thesis, Delft University of Technology, the Netherlands.*
- Moses, D.M. and H.G.L. Prion. 2004. *Stress and failure analysis of wood composites: a new model. Composites Part B Engineering, 35:251-261. DOI: 10.1016/j.compositesb.2003.10.002.*
- Sandhaas, C. 2012. *Mechanical behaviour of timber joints with slotted-in steel plates. PhD thesis, Delft University of Technology, the Netherlands.*
- Sandhaas, C., G. Ravenshorst, H.J. Blaß and J.W.G. van de Kuilen. 2013. *Embedment tests parallel-to-grain and ductility aspects using various wood species. European Journal of Wood and Wood Products, 71(5):599-608. DOI: 10.1007/s00107-013-0718-z*
- Sandhaas, C. and J.W.G. van de Kuilen. 2016. *Strength and stiffness of timber joints with very high strength steel dowels. Engineering Structures 131:394-404. DOI: 10.1016/j.engstruct.2016.10.046.*